Experimental Study of Nonequilibrium Expanding Flows

ROBERT E. DUFFY*

Rensselaer Polytechnic Institute, Troy, N. Y.

An experimental study of nonequilibrium expanding flows has been carried out by measuring the static pressure at several axial locations in a 30° included angle conical nozzle attached to the reflected end of a combustion driven shock tube. In the axial survey, measurements were made at locations corresponding to geometric area ratios of from 36 to 576. Reservoir stagnation conditions were: 1000 psia, 1350°K; 450 psia, 4000°K; and 250 psia, 7000°K. The test gases used in this study were dry room air, extra-dry analyzed air, and a high-purity mixture of 80% nitrogen and 20% oxygen. The data reduction procedures that have been employed in this study are discussed. The methods for treating effects due to boundary-layer growth both on the nozzle walls and on the static-pressure probe, static-pressure probe size, flow gradients in the nozzle, etc., are outlined. It has been found that corrections for these effects are necessary to interpret properly static-pressure data. The apparent disagreement between previous experimental investigations and theoretical analyses is traceable in a large measure to these corrections. The measurements are compared with results obtained using a one-dimensional analysis that incorporates a gas kinetic model based on the best available chemical data. It is shown that the experimental data are in good agreement with the theoretical results.

Introduction

IN recent years a considerable effort has been directed toward attempts to understand the manner in which the chemical kinetic reactions that are possible in a gas may couple with the fluid dynamic equations. The general category of problems involving such a coupling is often described by the term "nonequilibrium flow."

The strong coupling between the chemical kinetic reactions and the gasdynamic equations can be illustrated by the following two specific examples:

1) To determine experimentally the high Mach number aerodynamic characteristics of hypersonic vehicles, it has been necessary, in general, to construct simulation facilities. In these facilities high Mach number flows can be obtained by the expansion of a gas through a nozzle from a suitable reservoir. If one attempts to simulate the in-flight temperatures, as well as the flow Mach number, the reservoir gas must be maintained at a high temperature. With the expansion of a high-temperature reservoir gas it is possible that the chemistry of the gas may not be capable of remaining in equilibrium with the local thermodynamic properties. Such nonequilibrium effects may cause significant changes in the test flow properties.

2) It is also known that the propulsive efficiency of a rocket nozzle at high flight Mach numbers is a strong function of whether or not the gas remains in chemical equilibrium during the expansion. For example, at a flight Mach number of 10 for a typical ramjet nozzle configuration, the thrust produced per pound of air drops from a value of 70, if the gas is in chemical equilibrium, to a value of 30, if the chemistry of the gas is frozen at its reservoir condition.

The initial analysis for determining the properties of expanding flows that are not in chemical equilibrium with the local thermodynamic properties was carried out by Penner.[1] In this analysis, the properties of expanding flows which were "near-equilibrium" or "near-frozen" were determined by the use of perturbation techniques about the equilibrium and chemically frozen values. More recently, Bray and Appleton[2, 3] and groups at the Cornell Aeronautical Laboratory[4, 5] and Stanford University[6] have presented methods of analyzing flows with complicated chemistry. Of particular note in the development of these methods is the concept of the sudden freezing point which was introduced by Bray[2] in an attempt to circumvent tedious mathematical calculations.

All the methods of analysis presented to date contain some approximations that are open to question. An important question is the accuracy to which the postulated chemical kinetic reactions correctly represent the flow chemistry. These reactions use experimentally-determined rate constants. Normally the forward rate constant is often determined from relaxation-time measurements behind a normal shock wave. The reverse rate constant is then inferred from the equilibrium constant and the forward rate. Experimental measurements of the reaction rates, in some instances, show data scatter of a factor of 10. Also the use of the equilibrium constant to describe the reverse reaction rate for an expanding gas that is far from equilibrium may be questionable.[7]

In an attempt to explore some of these questions, an experimental study has been initiated at Rensselaer Polytechnic Institute to investigate the nonequilibrium character of expanding flows. It can be shown[4] that the species concentrations, static pressure, and static temperature of an expanding flow are sensitive to the degree of chemical nonequilibrium. In this study, static pressure has been measured and used as the indicator of nonequilibrium effects. Static pressure measurements have been used by Wegener,[8] Nagamatsu, Workman, and Sheer,[9, 10] and Hurle, Russo, and Hall[11] in studying the nonequilibrium character of expanding flows. In particular, the data presented in Refs. 9 and 10 are par-

Presented as Preprint 64-39 at the AIAA Aerospace Sciences Meeting, New York, January 20–22, 1963; revision received September 23, 1964. This research has been supported by the Office of Aerospace Research, U. S. Air Force, Contract No. AF 33(616)-7312. The material reported herein is taken in part from a thesis to be submitted in partial fulfillment of the requirements for the degree of Doctor of Philosophy in the Department of Aeronautical Engineering and Astronautics at Rensselaer Polytechnic Institute. The author wishes to acknowledge his indebtedness to H. T. Nagamatsu for suggesting this problem and for his stimulating discussions in the early phase of this study, and to H. S. Glick for his valuable criticisms and suggestions in the later phases of this program. The author is also indebted to those graduate students of the Department of Aeronautical Engineering and Astronautics at Rensselaer Polytechnic Institute whose combined efforts made the gathering of this experimental data possible.

* Assistant Professor of Aeronautical Engineering. Member AIAA.

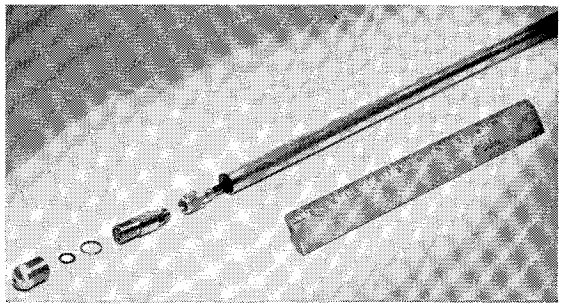

Fig. 1 Impact-pressure probe ($\frac{3}{4}$-in. diam).

ticularly relevant to the results of this present paper. In an experimental study reported by Nagamatsu, Workman, and Sheer,[10] they concluded that the static-pressure distributions measured along the axis of a hypersonic nozzle "do not agree with nonequilibrium calculations." The results of the present paper are in contradiction to this conclusion.

Experimental Facility

The studies of nonequilibrium expanding flows reported herein were conducted in a 30° included angle conical nozzle attached to the reflected end of a combustion driven shock tube. The nozzle consists of three sections: a stainless-steel interchangeable throat, a chrome-moly section that expands the flow to a 5.36-in. diam., and a machined cast aluminum section that expands the flow to an exit diameter of 12.28 in.

The interchangeable stainless-steel nozzle throats have been constructed with throat sections that have a constant radius of curvature and are faired tangentially into the 15° half-angle conical expansion section.

The driven section of the shock tube is fabricated of stainless-steel pipe with a 2-in. internal diameter. The length of the driven tube is 53 ft. The combustion driver is fabricated of chrome-moly steel and has an internal diameter of 3 in. Its length is 10 ft. Complete details as to the description and operation of this facility are given in Refs. 12 and 13.

Calculation of Nozzle Flow

In the case of a kinetically-complicated test gas such as air, the calculation of the nozzle flow properties, including nonequilibrium effects, is a complicated task. The strong coupling between the chemical rate processes and the fluid dynamics of the flow presents such difficulty that detailed numerical solutions must be carried out, even if one adopts stringent simplifying approximations.

One can, however, quickly determine the limits that the nozzle-flow properties may have in an expansion from a known set of reservoir conditions. Using the approximations that diffusion and viscous effects are small and that the flow is adiabatic and quasi-one-dimensional, simple standard procedures are available for obtaining the fluid properties in the limiting cases. On the one extreme, the flow can be considered to expand from the reservoir conditions while maintaining thermal and chemical equilibration. During this type of expansion, the energy that is tied up in the vibrationally- and chemically-active species of the gas is transferred into the translational and rotational modes of the flow. In contrast with this type of expansion, one can consider the case in which the chemically-active species remain frozen at their reservoir mass fractions. In this expansion process, only the translational, rotational, and vibrational degrees of freedom are equilibrated, and the energy in the chemically active species is not available for transfer. If, in addition to the freezing of the chemically active species, one considers the vibrational degrees of freedom to be frozen also, the expansion of the gas from the reservoir occurs at a constant value of the specific heat ratio.

Reservoir temperature conditions are established by the measurement of two quantities: 1) the shock speed past two stations that are 1 ft apart and located immediately upstream of the nozzle diaphragm, and 2) the initial pressure and temperature in the driven tube. For shock Mach numbers less than 5.0 in air, Ref. 14, with suitable correction for vibrational effects, is used to calculate the reservoir conditions after the shock-wave reflection. Above shock Mach numbers of 5.0, the equilibrium gasdynamic charts of Ref. 15 are used. Driven tube pressures behind the incident and reflected shock wave are measured with Kistler piezo-electric pressure transducers (Model 401). The uniformity of reservoir conditions has been discussed in Ref. 13.

In calculating the nozzle flow properties for the equilibrium expansion of air, Ref. 14 is used when reservoir temperatures are under 2000°K. Above this temperature, Mollier charts, similar to that of Ref. 15, are employed. More recently, charts have been developed giving the flow properties of air in equilibrium in hypervelocity nozzles.[17, 18]

Properties of the frozen expansions have been calculated in the manner presented in Ref. 17. This reference has also tabulated graphically the flow properties for a limited number of frozen expansions.

For a few specific sets of reservoir conditions, the tabulated results of nonequilibrium calculations, which have used the chemical kinetic model postulated by the Cornell Aeronautical Laboratory,[4] have been made available to the author by Geiger[19] and Lordi.[20]

Impact-Pressure Probe

The type and manner of construction of the impact probe used in this study was, to a large extent, determined by the impact pressure levels expected. For the range of reservoir temperatures and pressures chosen, calculations indicated that the lowest impact pressure level expected in an $M = 10$ nozzle was approximately 0.10 psia. At this pressure level, it was felt that a standard piezo-electric gage, such as the Kistler pressure transducer (Model 401), could be utilized.

An impact-pressure probe was constructed which used this transducer as a pressure-recording element. This pressure transducer was screwed into a brass hemispherical impact head that was 0.75 in. in diameter. The impact head, in turn, was screwed into a 0.75-in. o.d. 36-in.-long stainless-steel rod. On the axis of the hemispherical head, a small hole was drilled (whose diametrical effect has been examined and discussed elsewhere in this report) to expose the pressure-recording face of the Kistler gage. A picture of this probe is shown in Fig. 1.

As constructed, this probe had an output of approximately 4.3 mv/psi. However, it should be noted that the output of the impact probe was not linear with pressure. This effect will be discussed in more detail later in this report.

Static-Pressure Probe

Inviscid calculations of the state properties of the gas in the nozzle indicated that the lowest static pressure that could be expected was 0.0005 psia for the range of reservoir temperatures and pressures chosen. This pressure was determined on the basis that the vibrational and chemical-kinetic properties of the gas were completely frozen at the reservoir conditions during the expansion. Any tendency for the flow to remain in equilibrium and the effects of boundary-layer development will increase the static pressure above this level of 0.0005 psia.

It was evident that a gage, such as the Kistler pressure transducer (Model 401), does not have sufficient output at low pressure levels to be employed for the measurement of static pressures. Static-pressure probes have been constructed which use as their pressure-transducer elements

Table 1 Static-pressure probe geometry

Probe diameter, in.	Piezo-electric crystals	Crystal element, no. and in.		Approximate output, mv/psi	Nose shape
$\frac{3}{8}$	Barium titinate	2	$\frac{1}{8} \times \frac{1}{8}$	8.5	4° cone-cylinder with large radius fairing
$\frac{1}{2}$	Lead-zirconate-titinate	2	$\frac{1}{8} \times \frac{1}{8}$	10.0	Tangent ogive
$\frac{3}{4}$	Barium titinate	2	$\frac{1}{8} \times \frac{1}{4}$	19.0	4° cone-cylinder with large radius fairing

either barium titinate or lead-zirconate-titinate piezo-electric crystals.

A crystal, as received from the manufacturer, is polarized with respect to its faces and is approximately $\frac{1}{8}$ in. in thickness. Crystal diameters of $\frac{1}{8}$ and $\frac{1}{4}$ in. have been used. In constructing a static-pressure probe, two crystals of equal diameter are electrically paralleled by gluing together the appropriate faces with air-hardening "Hanovia" silver paint. This composite element, with output leads attached, is then mounted in a brass shell and firmly secured with epoxy resin such that one face of the element is flush with the end of the shell. Care must be taken so as to prevent any section of the element from making contact with the brass shell. As now mounted, only one face of the element will be exposed to the test gas. A very thin film of epoxy resin is painted across this face. The purpose of this coating is to prevent damage to the element face due to possible exposure to a high-temperature or a high-humidity atmosphere.

This brass shell is then imbedded in the center of a larger cylindrical pressure-sensing unit and is supported in place by filling the gap between the unit and the brass shell with General Electric RTV-11 silicone rubber. Extreme care must be taken to assure that the brass shell containing the sensing element is isolated from the pressure-sensing unit by means of a layer of silicone rubber. The unit has 12 equally spaced holes drilled normal to its outside surface. These holes, when they coalesce, form an internal cavity. The brass shell containing the sensing element is positioned within the unit so that the face of the pressure-sensitive element is exposed to this cavity.

The forward end of the unit is step-reduced in diameter and threaded so as to allow the attachment of a long slender nose. The rear of this unit is likewise step-reduced in diameter and threaded. This construction allows the element to be screwed into a hollow stainless-steel rod through which the output leads from the pressure-sensing element may be channeled. The outside diameter of the stainless-steel rod, pressure unit, and the aft section of the nose cone is constant. A close-up view of a $\frac{3}{4}$ in. diam pressure unit is shown in Fig. 2.

Three static-pressure probes have been fabricated to date. Their general characteristics are described in Table 1. A view of these static-pressure probes is shown in Fig. 3.

Static and Impact Probe Calibration

The manner in which a probe must be calibrated depends to a large extent on the time constant of the pressure-sensing element which is used. For example, the Kistler pressure transducers (Model 401) are capable of being calibrated statically principally because the electronic circuitry can be constructed using d.c. amplifiers. Conversely, barium titinate and lead-zirconate-titinate crystals used in this study have such low outputs that a.c. amplifiers have been employed. Hence, the static-pressure probes must be calibrated using dynamic techniques.

For calibration of the static-pressure probes the technique chosen was to subject the probe to a pressure pulse obtainable from the passage of a weak shock past the hole openings in the pressure-sensing unit. If the initial pressure before the passage of the shock is known, as well as the shock Mach number, one can, using perfect fluid theory, calculate the pressure jump across the shock. The use of perfect fluid theory to determine the pressure jump is valid when the shock Mach number is small. In practice, this technique has proven to be so simple that it was decided to calibrate the impact probe in a similar manner.

In the initial phases of this study, the impact- and static-pressure probes were calibrated in the driven tube of the hypersonic shock tunnel. The shock tunnel was modified so as to reflect fully the flow at the end of the driven tube. An impact or static probe was then mounted in the center of the driven tube and a weak shock passed over the probe. The passage of this shock over the probe provided the dynamic calibration of the output of the probe in terms of the pressure jump across the shock.

The weak shock was generated by modifying the shock tunnel driver so as to enable the diaphragm separating the driver from the driven tube to be broken manually. The diaphragms were broken by cutting them with an X-shaped cutter that could be moved longitudinally along the axis of the driver. The diaphragms used in these calibration tests were made from household-grade aluminum foil.

In this series of calibration tests, the impact probe was positioned either at the reflected end of the driven tube or at a sufficient distance upstream such that the secondary pressure pulse caused by the shock-wave reflection from the end of the driven tube did not influence the calibration.

The static probe was always calibrated on the pressure jump of the incident shock. Because of the geometry of the static pressure probe it was felt that the calibration of this probe by the reflected technique may introduce serious errors.

During the later stages of this investigation, an 8-in. diam shock tube became available. The details of this shock tube are described in Ref. 13. A recalibration of all impact and static probes was undertaken using this facility. Agreement between the two sets of calibration data is excellent.

In view of the fact that the impact and static probes were to be used to record low pressures, one must determine whether the probes do, in fact, have the ability to measure the correct

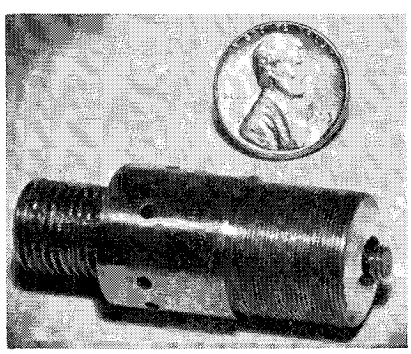

Fig. 2 Static-pressure unit ($\frac{3}{4}$-in. diam).

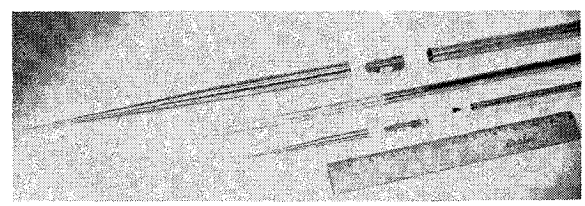

Fig. 3 Static-pressure probes.

pressure. It is well known that at low pressures viscous effects are important. In particular, one could reason that large viscous effects in the probe-inlet holes may retard the flow into the cavity that contains the pressure-sensing element; thus the pressure in the cavity may not be equal to the pressure at the inlet. In an attempt to find the effect of hole size on the performance of a probe, a series of calibration tests were conducted. In these tests the hole size of the impact and static probes was enlarged by small increments, while the pressure jump ranged from 0.001 to 1.20 psia. The hole diameter in these tests varied from 0.020 to 0.125 in.

At any fixed pressure level, the ultimate output of a probe was independent of hole size. However the rise time of the probe (time necessary to produce a steady-state output) is a strong function of hole size. This result is not unexpected. What is of importance is that the rise time of the impact- and static-pressure probes at pressure levels that are expected in the nozzle can be determined. Hole diameters were chosen so that the rise time of a probe, when subjected to the lowest pressure expected in the nozzle, was less than 350 μ sec. At less critical pressure levels, the rise times average about 50 μ sec.

It has also been observed that, for a given pressure pulse across the probe, the rise time decreased as the initial pressure level increased. Hence, one can anticipate that these probes, when used in the nozzle, can respond much faster to subsequent pressure pulses than it can to the flow-initiating pressure pulse.

The acceptable rise time that an impact- or static-pressure probe must possess is in effect determined by the uniformity of the reservoir conditions. For reservoir conditions that vary appreciably over the testing period, one must use probes with fast rise times. Conversely, with slowly-varying reservoir conditions, one can tolerate much larger rise times for the probes. Unfortunately, one cannot continue to enlarge hole size with the hope of decreasing the rise time. As the hole size is increased, a point is reached where the output signal from the gage shows a large amplitude random-noise signal. This random noise has been attributed to internal noise generated between the crystal and its housing when it is subjected to a rapid variation in pressure. This effect is much more pronounced on the static probes than on the impact probe. When large hole diameters are used on the static probe, one can eliminate the random-noise effect merely by sealing over the inlets of a number of the holes. This observation supports the conclusion that the noise is generated by the rapid variation in loading pressure on the crystal.

The results of this calibration study have shown that at high pressures (above 1.00 psia for the impact probe and 0.25 psia for the static probe) the output of each probe is linear with pressure. At very low pressures this linearity does not exist. Typical dynamic calibration traces of the outputs of these probes are shown in Ref. 16.

Spurious signals, due to any vibration of the impact or static pressure probe induced by the flow starting process in the nozzle, have been minimized by attaching the probes to a lead-weighted model-support sting through a rubber vibration-isolation unit.

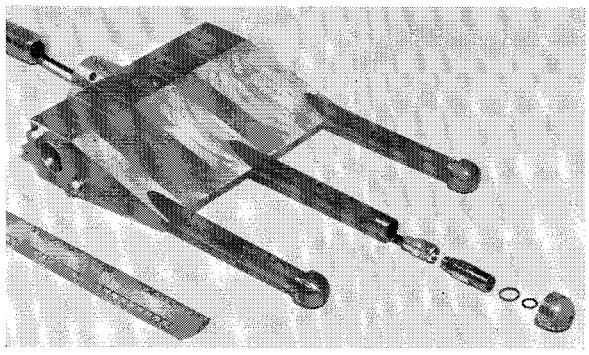

Fig. 4 Impact-pressure rake.

Transverse Gradients in the Nozzle

To assess the transverse uniformity of the flow in the nozzle, a series of tests were conducted to establish the off-axis impact pressure. An impact-pressure rake was constructed which could simultaneoulsy record the impact pressure at a discrete number of points along a diametrical line. This rake is shown in Fig. 4, and the details of construction are given in Ref. 13.

This same rake has been used to establish any changes, in the nozzle flow properties, due to the insertion of an on-axis static-pressure probe. By replacing the on-axis impact-pressure head of the rake with a static-pressure probe and by observing the change in impact pressure at a fixed off-axis location, the net effect of the static probe in altering the flow properties can be determined. This technique allows one to determine the combined effects due to 1) the static-pressure probe cross-sectional area, 2) the boundary-layer growth on the static probe, and 3) any mutual interaction between the boundary-layer growth on the static-pressure probe and on the nozzle wall.

Impurity Levels

In the early stages of this study, absolute impurity levels of the test gas were unknown. The test gas was ordinary compressed room air that had been dried to a dew point of $-40°$F. No attempt was made to assess the possible contamination of the test gas due to any uncleanliness of the driven-tube walls or due to impurities that may be present in the driven-tube loading lines. The driven tube was prepared for loading with the test gas by first purging it with dry air to eliminate any water vapor. The tube was then pumped down to approximately 1 mm Hg and loaded with the test gas to a pressure well in excess of the desired pressure. A second evacuation reduced the driven-tube pressure to the desired level.

The measurement of impact and static pressures along the axis of the nozzle, for a fixed reservoir temperature and pressure, indicated that, for some of the reservoir conditions chosen, the flow appeared to be expanding in an equilibrium manner. However, nonequilibrium flow calculations for the same reservoir conditions have indicated that there is a departure from equilibrium.[19] It was felt that the differences between the measured and calculated results were more than could be attributed to experimental error. Thus, a re-examination of the possible effects of impurities in the driven-tube test gas was conducted.

To reduce the impurity contribution caused by gas remaining in the driven tube prior to loading, the vacuum integrity of the driven tube has been improved to such an extent that at the lowest initial loading pressure the maximum impurity content is less than one part in ten thousand. The initial pressure of the driven tube is less than 1 μ of mercury prior to loading. The leak rate is 0.02 μ Hg/min. Between the time the driven tube is loaded with the test gas and the time the test occurs, a change in pressure is not detectable on a silicone-oil micromanometer. It is expected that the major gas impurity in the driven tube is room air.

The test gases, as received from the storage cylinders, are now analyzed on a mass spectrometer and the concentrations of the gaseous species determined.

To prevent contamination of the test gas by nongaseous impurities that may deposit on the tunnel walls, the driven tube is scrubbed after each experiment by passing alternately clean dry lintless cloths and lintless cloths soaked in acetone through the tube. The nozzle walls are scrubbed clean prior

to a test to reduce the possibility of contamination caused by impurities on these surfaces.

Dry ice and acetone cold-traps and baffling are used on all vacuum pumps to prevent back-gassing of pump oil. A similar cold trap is also installed in the gas-loading line of the driven tube.

Test Results

The experimental investigation was conducted in a 30° included angle conical nozzle. The throat diameter was 0.50 in. which, for a perfect-gas expansion, produces a nominal flow Mach number of 10 at the nozzle exit.

Axial surveys of impact and static pressure have been obtained in the Mach 10 nozzle over a range of reservoir temperatures and pressures. Room air, dry analyzed air, a mixture of 20% oxygen and 80% nitrogen, high-purity nitrogen, and commercial oxygen have been used as test gases. Only the results of the tests in which air was used as the test medium will be reported here.

The reservoir pressure and temperature conditions for the series of axial pressure measurements in air have been fixed at 1000 psia, 1350°K; 450 psia, 4000°K; and 250 psia, 7000°K.

For the proper interpretation and comparison of static pressure measurements with predicted static-pressure values obtained from inviscid, nonequilibrium, one-dimensional flow calculations, it is necessary to incorporate into the measured data numerous corrections. A detailed discussion of the corrections to the data that must be considered is given in Ref. 16. It is necessary, for example, to consider the boundary-layer growth along the nozzle walls in the expanding, high Mach number flow. Hence, even though the static-pressure probes are positioned at a point in the nozzle which corresponds to a geometric cross-sectional area ratio, the results of the measurement at this point must be analyzed in terms of the effective area ratio. In addition, the one-dimensional concept inherent in the numerical calculations may not be realized for highly divergent nozzles, and the association of a cross-sectional area with the axial pressure measurements may be in error.

Other investigators who have employed conical nozzles in similar hypersonic facilities have indicated that the boundary-layer growth along the nozzle walls has a contouring effect on the nozzle flow. To ascertain this contouring effect in the Mach 10 nozzle, an impact rake was installed in the nozzle and simultaneous measurements of the impact pressure at discrete points across the nozzle diameter were obtained. If the nozzle expansion is conical, then as one moves off the axis in a plane that is transverse to the nozzle axis, a decrease in impact pressure will occur. Rake measurements were made at the axial station corresponding to the section that has a 12-in. diam. The rake survey covered approximately the central 8 in. of this section. The maximum variation in the mean value of the impact pressure between the centerline value and points 4 in. off the axis was 3.2%. This difference is less than the measuring accuracy of the impact probe. Hence, no quantitative values can be assigned to the contouring effect of the wall boundary layer. The apparent small variation of impact pressure in the transverse plane supports the assumption that the flow may be considered as approximately one-dimensional.

The effective nozzle cross-sectional area that must be associated with a particular axial measurement is determined by recognizing that the impact pressure recorded by the probe is fixed by the passage of the freestream flow through the detached shock ahead of the probe. Since there are longitudinal gradients in the flow properties, the impact pressure recorded must be associated with an area corresponding to the position of the detached shock in the nozzle and not with a test section area corresponding to the inlet opening in the impact probe. To find the shock-detachment distance, the method of Ref. 21 is used. It is assumed in the calculation of the shock-detachment distance that the flow is in equilibrium on both sides of the shock.

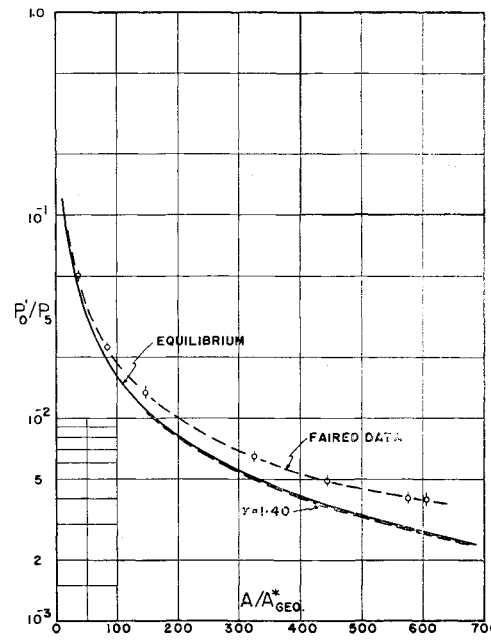

Fig. 5 P_0'/P_5 vs $(A/A^*)_{GEO}$. Air reservoir conditions: P_5 = 1000 psia and T_5 = 1350°K.

One can determine an effective area ratio by knowing the ratio of the impact pressure to the reservoir pressure and the reservoir conditions. From the effective area ratio at different longitudinal positions in the nozzle, the effective radius of the uniform inviscid core can be found. The effective displacement thickness of the boundary layer may then be determined as the difference between the actual nozzle radius and the effective radius of the inviscid core. The results of a typical axial impact-pressure survey, corresponding to reservoir conditions of 1000 psia and 1350°K, are shown in Fig. 5. The boundary-layer displacement thickness, for these reservoir conditions, using the foregoing method of data reduction is shown in Fig. 6. The displacement thickness distributions at other reservoir conditions have similar shapes.

With the knowledge of the effective area ratio, inferred from the impact-pressure measurements, correlations of the measured and calculated static pressures may be made. In making this comparison a further correction is incorporated into the effective area ratio to account for the insertion of the static-pressure probe into the flow field. In general, the placement of a static-pressure probe into the flow field is expected to change the effective area ratio. This effective area ratio change is the sum of three effects that are due to 1) the static-pressure probe cross-sectional area, 2) the boundary-layer development along the probe, and 3) the mutual interaction between the probe and the nozzle wall boundary layer. The sum of these effects in changing the effective area ratio has been established by using an impact- and static-pressure

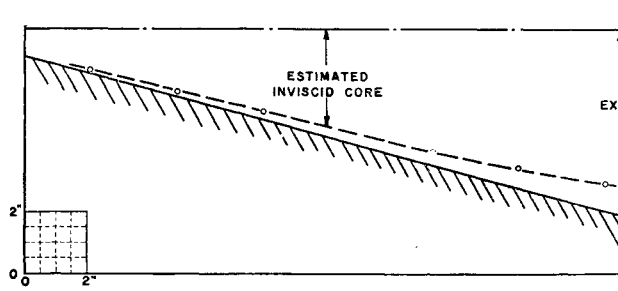

Fig. 6 Boundary-layer displacement thickness, reservoir conditions: P_5 = 1000 psia, T_5 = 1350°K.

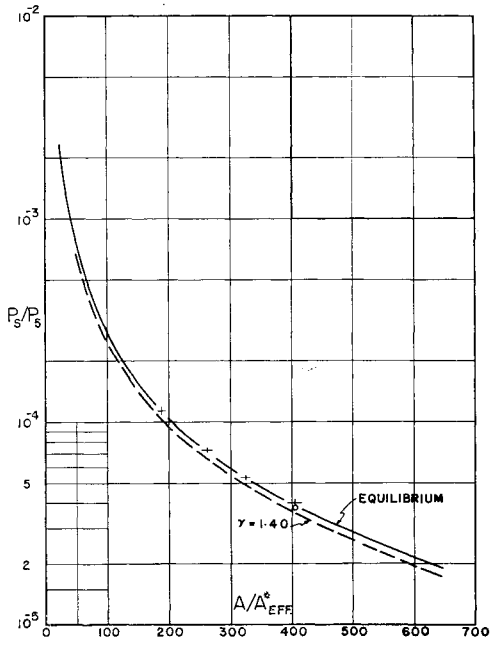

Fig. 7 P_s/P_5 **vs** $(A/A^*)_{eff}$. **Air reservoir conditions:** P_5 = **1000 psia,** T_5 = **1350°K,** L = **2.84 cm.**

rake described previously. Measurements with the impact- and static-pressure rake indicate that, for the reservoir conditions chosen, the viscous effects, due to either the probe boundary layer or the mutual interaction between the probe and nozzle wall boundary layers, are relatively small. The decrease in the effective area ratio inferred from the impact measure varied between 5 and 9%. The worst case encountered was with the $\frac{3}{4}$ in.-diam static-pressure probe located at a 12-in.-diam test section and with the 4000°K reservoir.

It has been suggested by some investigators[11] that static-pressure probes of the type described herein may be subject to large viscous interaction effects. An estimation of the maximum change in static pressure due to this effect has been determined by calculating the induced pressure on a probe that is situated in a uniform stream whose Mach number and Reynolds number is taken to correspond with the 12-in.-diam station in the nozzle. As one makes measurements further upstream in the nozzle, the Mach number decreases and the Reynolds number increases, so that the effect of viscous interaction will decrease rapidly. These calculations result in an induced pressure change of 5, 7, and 2.5% at the 12-in.-diam station for the reservoir conditions of 1350°, 4000°, and 7000°K, respectively. The mean value of the static pressure measurement at the 12-in.-diam station incorporating this viscous interaction correction is shown by the small circle in Figs. 7–9.

Three static-pressure probes with different diameters have been tested at the same reservoir conditions in a manner such that the inlet holes are at the same geometric cross-sectional area ratio. Within the measuring ability of these probes, the pressure recorded was the same. These probes are considered to have the ability to record pressure within a maximum error of 5%.

Axial static-pressure measurements correlated on the basis of the effective area ratio for three different reservoir conditions are shown in Figs. 7–9. The reservoir conditions for these figures are 1000 psia, 1350°K; 450 psia, 4000°K; and 250 psia, 7000°K, respectively. The vertical bars on the data indicate the limits of scatter in the static pressure measurements; whereas the horizontal bars show the effect of scatter in the impact pressure measurements and the interpretation of an effective area ratio from these measurements. These results have all been taken using room air as the test gas. As mentioned previously, impurities and their concentrations in the experiments are unknown.

To determine the influence of gas-impurity levels on these results, a series of control experiments were made using a clean driven tube. The test gas used was air with a dew point of −70°F. This air has been analyzed for concentrations of hydrogen, carbon monoxide, carbon dioxide, argon, nitrogen, and oxygen. The results of this analysis are, by volume, O_2 = 20.9%, CO_2 = 44 ppm, A = 0.90%, CO = less than 10 ppm, H_2 = 1070 ppm, and N_2 = balance. The axial location where this impurity check was made is the 12-in. diam test section. A large diameter test section was chosen since it was felt any differences due to gas impurity would be most evident at the larger area ratios. For reservoir conditions of 1000 psia, 1350°K and 450 psia, 4000°K, no measurable differences in the static pressure were observable. At the 7000°K reservoir temperature, this controlled impurity check, as yet, has not been made.

It is apparent from the results presented in Figs. 7–9 that at reservoir conditions of 1000 psia and 1350°K the gas expands in the nozzle under conditions that are closely represented by the equilibrium curve. At reservoir conditions of 450 psia, 4000°K and 250 psia, 7000°K, nonequilibrium expansions occur.

The reservoir conditions of 1000 psia, 1350°K have been purposely chosen so as to provide a proper control experiment. For this set of reservoir conditions, the reservoir energy that is contained in any vibrational- or chemical-active degrees of freedom is less than 6.5% of the total reservoir energy. One would expect, therefore, that, if any nonequilibrium effects could occur during the nozzle expansion process, the net change in the gasdynamic flow properties would be exceedingly small; i.e., for all intensive purposes the gas can be considered to expand from the reservoir under essentially equilibrium conditions. Thus, this solution provides one with a check on the ability to measure physically the axial variation in static pressure and to properly interpret the static pressure measurements.

Assuming reservoir conditions of 500 psia and 4000°K, the results of a nonequilibrium calculation of the static-pressure variation in a nozzle, using the method detailed in Ref. 4, are shown in Fig. 8. This numerical calculation assumed that the gas was vibrationally equilibrated. The chemical-

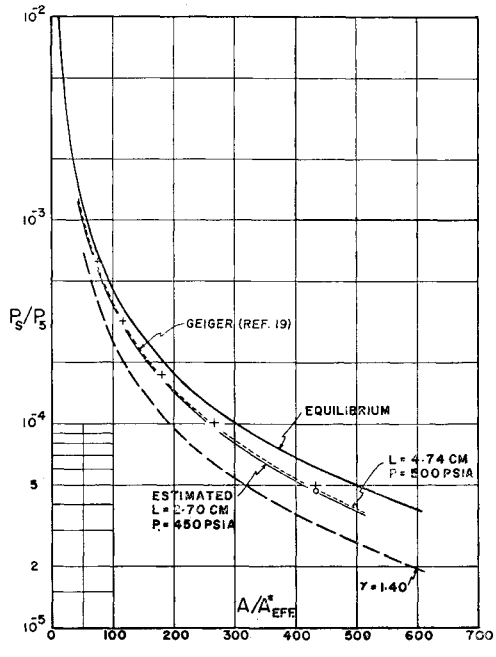

Fig. 8 P_s/P_5 **vs** $(A/A^*)_{eff}$. **Air reservoir conditions:** P_5 = **450 psia,** T_5 = **4000°K,** L = **2.70 cm.**

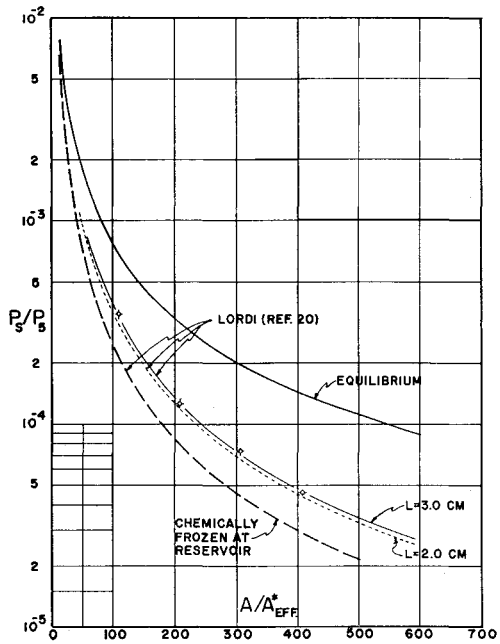

Fig. 9 P_s/P_5 **vs** $(A/A^*)_{\text{eff}}$. **Air reservoir conditions:** P_5 = **250 psia,** T_5 = **7000°K,** L = **2.75 cm.**

kinetic gas model and the reaction rates used in this analysis are given in Ref. 4. These results have been obtained from Ref. 19. In this nonequilibrium analysis, the nozzle geometry was assumed to have a 1-in. diam throat with a 30° included angle conical expansion section. The area distribution used in the nonequilibrium analysis was mathematically expressed as a hyperbolic function in terms of the distance downstream of the throat and a scaling length. The value of the nonequilibrium scaling length ($L = D^*/2 \tan\theta$) corresponding to this nozzle is 4.74 cm. In the present nozzle configuration, the scaling length based on a geometrical wall angle is 2.37 cm. From a knowledge of the displacement thickness of the wall boundary layer, an effective expansion angle may be determined. The scaling length, based on an effective expansion angle, is 2.70 cm. As indicated in Ref. 5, the static-pressure variation is sensitive to a parameter that is the product of the reaction rate and the scaling length. The dominant factor in determining the level of the static-pressure variation during an expansion is thus expected to be the three body recombination reaction for which one can consider the thermodynamic properties to scale according to a correlating parameter $\rho^2 L$ = const. By using some tabulated results from Ref. 5, it is estimated that the static pressure will be about 3 to 4% lower for the present reservoir conditions and nozzle geometry than for a reservoir pressure of 500 psia and a scaling length of 4.74 cm. The predominant chemical reaction that controls the level of the static pressure during this expansion process is principally the three body recombination of atomic oxygen. Nitrogen dissociation is unimportant at these reservoir conditions.

For the reservoir conditions of 250 psia and 7000°K, nonequilibrium calculations have been obtained from Ref. 20. The comparison between the calculated and measured static pressures as a function of the effective area ratio is shown in Fig. 9. Also shown are the results of a series of calculations giving the variation in static pressure when the expansion process occurs in equilibrium and when the chemically-active species are frozen at the reservoir conditions. The kinetic gas model used was the same as previously indicated with vibrational equilibration assumed during the expansion. Analysis of the gas chemistry for expansion from this reservoir condition indicates an interesting effect. For a 250 psia, 7000°K reservoir the fraction of the stagnation enthalpy in the atomic oxygen and nitrogen species is almost equal. During the expansion, freezing of atomic oxygen occurs very close to the nozzle throat. However, atomic nitrogen is equilibrated to molecular nitrogen through the NO exchange reactions. Thus these exchange reactions play an important role in governing the static-pressure level.

It is evident from Fig. 9 that, in the case in which the nonequilibrium and equilibrium solutions differ substantially, the agreement between the nonequilibrium solution and experiment is excellent. This agreement is also seen for the 450 psia, 4000°K reservoir in Fig. 8.

Conclusions

The experimental results in air are in agreement with calculations obtained from a theoretical analysis that assumes a large number of chemical reactions and the best available reaction rate data. This experimental confirmation of the theoretical analysis indicates that the assumed chemical model appears to predict satisfactorily the static-pressure distribution of an expanding flow in the range of the present experiments (i.e., from reservoir conditions of 1000 psia, 1350°K to 250 psia, 7000°K). Therefore, it is believed that this theoretical model can be used with some assurance in calculations of other thermodynamic and chemical properties.

References

[1] Penner, S. S., *Introduction to the Study of Chemical Reactions in Flow Systems* (Butterworths Scientific Publications, Ltd., London, 1955).

[2] Bray, K. N. C., "Atomic recombination in a hypersonic wind-tunnel nozzle," J. Fluid Mech. **6**, 1–32 (1959).

[3] Bray, K. N. C. and Appleton, J. P., "Atomic recombination in nozzles: methods of analysis for flows with complicated chemistry," Univ. of Southampton, Rept. 166 (April 1961).

[4] Eschenroeder, A. Q., Boyer, D. W., and Hall, J. G., "Exact solutions for nonequilibrium expansions of air with coupled chemical reactions," Cornell Aeronautical Lab. Rept. AF-1413-A-1 (May 1961); also Phys. Fluids **5**, 615 (1962).

[5] Hall, J. G., Eschenroeder, A. Q., and Marrone, P. V., "Inviscid hypersonic airflows with coupled nonequilibrium processes," Cornell Aeronautical Lab. Rept. AF-1413-A-2 (May 1962).

[6] Vincenti, W. G., "Calculations of the one-dimensional nonequilibrium flow of air through a hypersonic nozzle," Stanford Univ., Interim Rept. (May 1961).

[7] Bauer, S. H., "Chemical kinetics: a general introduction," *AIAA Progress in Astronautics and Rocketry: Hypersonic Flow Research* (Academic Press, New York, 1961), Vol. 7, pp. 143–172.

[8] Wegener, P., "Supersonic-nozzle flows with a reacting gas mixture," Phys. Fluids **2**, 264–275 (1959).

[9] Nagamatsu, H. T., Workman, J. B., and Sheer, R. E., "Hypersonic nozzle expansion with air atom recombination present," J. Aerospace Sci. **28**, 833–837 (1961).

[10] Nagamatsu, H. T. and Sheer, R. E., "Vibrational relaxation and recombination of nitrogen and air in hypersonic nozzle flows," AIAA Preprint 64–38 (January 1964).

[11] Hurle, I. R., Russo, A. L., and Hall, J. G., "Experimental studies of vibrational and dissociative nonequilibrium in expanding gas flows," AIAA Preprint 63–439 (August 1963).

[12] Duffy, R. E. and Rogers, D. F., "Design and characteristics of a small hypersonic shock tunnel combustion driver," Aeronautical Research Lab., U. S. Air Force Rept. ARL-62-307 (March 1962).

[13] Chang, Z. S., Duffy, R. E., Hoppmann, R. F., Rogers, D. F., Sundaram, T. R., and Glick, H. S., "Research on hypersonic rarefied viscous flow phenomena and magnetohydrodynamics at extremely high Mach numbers and temperatures," Aeronautical Research Laboratory, U. S. Air Force Rept. ARL 64-5 (January 1964).

[14] Ames Research Staff, "Equations, tables, and charts for compressible flow," NACA Rept. 1135 (1953).

[15] Feldman, S., "Hypersonic gas dynamic charts for equilibrium air," Avco Research Lab. Rept. 40 (January 1957).

[16] Duffy, R. E., "A static pressure measurement technique for chemical kinetic studies," Proceedings of the First International Congress on Instrumentation in Aerospace Simulation Facilities, pp. 23-1–23-18 (September 1964).

[17] Yoshikawa, K. K. and Katzen, E. D., "Charts for air flow properties in equilibrium and frozen flows in hypervelocity nozzles," NASA TN-D-693 (April 1963).

[18] Jorgensen, L. H. and Baum, G. M., "Charts for equilibrium flow properties of air in hypervelocity nozzles," NASA TN-D-1333 (September 1962).

[19] Geiger, R., "Nonequilibrium solution for reservoir conditions of 500 psia, 4000°K, L = 4.74 cm," private communications, General Electric Missile and Space Vehicle Div., Valley Forge, Pa. (August 1963).

[20] Lordi, J., "Nonequilibrium solution for reservoir conditions of 250 psia, 7000°K, L = 2.0 and 3.0 cm.," private communications, Cornell Aeronautical Labs., Buffalo, N. Y. (October 1963).

[21] Lobb, R. K., "Experimental measurements of shock detachment distances on spheres fired in air at hypervelocities," Specialists' Meeting on the High Temperature Aspects of Hypersonic Flow, Brussels (April 3–6, 1962).

Linear Pyrolysis of Thermoplastics in Chemically Reactive Environments

ROBERT F. MCALEVY III* AND JAMES G. HANSEL†
Stevens Institute of Technology, Hoboken, N. J.

The surface pyrolysis rate of two common thermoplastics, polystyrene (PS) and polymethylmethacrylate (PMM), has been measured in inert and chemically reactive environments, using the exhaust gas of a small rocket motor as a source of intense surface heating. Small plastic beads were employed to fabricate porous plastic specimens through which metered quantities of ten selected gases individually were passed; this novel porous plug technique permitted close experimental control of test gas concentration at the site of degradation. At a constant surface heating exposure (approximately 20 cal/sec-cm^2) the pyrolysis rate of PMM was unaffected by all ten, whereas that of PS was accelerated equally by both Cl_2 and NO_2. It is hypothesized that the acceleration is a result of Cl and NO_2 substitutions in the PS chains, primarily at the tertiary hydrogen locations, thereby creating "weak links" that enhance thermal degradation. In direct conflict with previous bulk degradation results of others, the presence of ClO_3F, O_2, and other less chemically reactive gases did not accelerate the surface degradation of PMM or PS; a rational basis for resolving this paradox is presented. Of considerable interest for propulsion applications is the implied invalidity of extrapolation of bulk degradation data obtained at very mild heating rates in chemically reactive environments to high surface heat flux conditions.

Background and Introduction

RECENTLY there has developed considerable interest in the linear pyrolysis (*surface* degradation due to intense surface heating) of thermoplastics, as the process has been incorporated in a pivotal way in current theories of solid propellant ignition[1, 2] and flame spreading,[3] as well as deflagration,[4–6] protective ablation of atmospheric re-entry vehicles,[7, 8] and hybrid (solid fuel) rocket motor combustion.[9, 10] Much speculation has centered on the possibility of chemically reactive gases in the surrounding atmosphere accelerating the pyrolysis rate either by attacking directly the decomposing polymer surface, or by exothermally reacting with polymer decomposition products in the gas phase to produce an increase in surface heating, or both. Evidence in support of this possibility is drawn from the results of widely used *bulk* degradation kinetics experiments as well as from laboratory experiences with each of the aforementioned phenomena, but all of these experiments suffer from inherent limitations that preclude elucidation of the role of the chemically reactive environment. These limitations are summarized in the following paragraph.

Thermogravimetric analysis (TGA) and differential thermal analysis (DTA), both bulk heating techniques, indicate that O_2 (apparently the only chemically reactive gas ever studied extensively) in the surrounding atmosphere usually produces an acceleration of the thermoplastic bulk degradation rate.[11–14] These techniques, as a result of relatively mild heating exposures, produce degradation rates less than one-thousandth of those of interest in propulsion applications, although the reactive gas concentration at the sample surface can be controlled quite accurately. On the other hand, much higher regression rates are obtained when, for example, a high energy arcjet[8] is employed as a source of intense surface heating in chemically reactive (O_2) and inert (N_2) environments. However, this technique, as well as attempts to examine the role of O_2 by experimenting with laboratory hybrid motors, cannot discriminate between degradation acceleration produced by direct attack on the polymer surface and that produced by heat feedback from nearby, gas phase, exothemic, chemical reactions with polymer vaporization products. Also, in this class of experiments, the reactive gas concentration at the polymer surface cannot be accurately controlled.

Presented as Preprint 64-86 at the AIAA Aerospace Sciences Meeting, New York, January 20–22, 1964; revision received November 12, 1964. This work was sponsored, in part, by the Office of Naval Research under Contract Nonr 263(48).

* Professor, Department of Mechanical Engineering, and Director of the Combustion Laboratory. Associate Fellow Member AIAA.

† Instructor, Department of Mechanical Engineering; now Research Staff Member, Department of Aerospace and Mechanical Sciences, Princeton University, Princeton, N. J. Member AAIA.